I2MTC 2008 – IEEE Instrumentation and Measurement
Technology Conference
Vancouver Island, British Columbia, Canada, May 12–15, 2008

A Label-free CMOS DNA Microarray based on Charge Sensing

E. Anderson[1,2], J. Daniels[1,2], H. Yu[2], T. Lee[1], N. Pourmand[2,3]

[1]Department of Electrical Engineering, Stanford University
161 Packard Building, 350 Serra Mall, Stanford, CA 94305
E–mail: erik.anderson@stanford.edu.

[2]Stanford Genome Technology Center
855 S. California Ave., Palo Alto, CA 94304

[3]Department of Biomolecular Engineering, University of California, Santa Cruz
1156 High St., Santa Cruz, CA 95064
E–mail: pourmand@soe.ucsc.edu.

Abstract – *The first label-free CMOS DNA polymerization sensor is reported. The 5-by-5 sensor array measures the charge induced on an electrode from a DNA fragment undergoing polymerization. Importantly, no post-processing is required as passivated top-metal electrodes are used. The measured limit of detection (with enzymatic buffer) is 25 fA for a one second integration time, or equivalently 25 fC of charge, although the limit set by the electronic noise is 3.5 times smaller. Using our chip, we demonstrate the detection of DNA polymerization. The sensor can be used to sequence short DNA segments in addition to detect DNA hybridization in microarrays.*

Keywords – *DNA microarray, CMOS, Charge Sensing*

I. INTRODUCTION

In recent years, DNA microarrays have become an important research tool in the biological and medical communities. DNA microarrays have allowed researchers to reconstruct metabolic pathways in cells, understand the progression of disease, and develop diagnostics and therapeutics. Conventional DNA microarrays, which use lasers and optics to detect fluorescent tags, are ill-suited for use in portable point-of-care medical systems. Researchers have been exploring various electronic DNA sensing techniques targeted to point-of-care medical diagnostics because they can be manufactured in high volumes at low-cost. These electrical-based techniques have sensed DNA hybridization by measuring a change in surface impedance [2, 8], surface charge using field-effect devices [1, 7], current from redox-cycling above an electrode [3], conductivity between two electrodes [4, 6], or conductivity of a giant magnetoresistance (GMR) spin valve in the presence of a magnetic nano-particle [5].

In this paper, we describe a 25 pixel label-free CMOS DNA microarray based on a charge sensing mechanism which detects DNA polymerization [9, 10]. Unlike the aforementioned electrical detection techniques, this charge-based technique could be used for both hybridization assays and sequencing short DNA segments.

II. SENSOR PRINCIPLE

As shown in Figure 1, a single-stranded DNA sequence, or an oligonucleotide, (the "probe") is immobilized above an electrode. When a complementary single-stranded sequence is introduced (the "target"), it hybridizes onto its corresponding probe. Polymerase enzymes are subsequently added along with the required free nucleotides needed for polymerization (the incorporation of free nucleotides into the second strand of a partially complete double-stranded DNA molecule). DNA synthesis (or polymerization) can be detected because the incorporation of a nucleotide (i.e. an "A," "T," "G," or "C") into the DNA molecule causes a net local charge increase of $1e^-$, balanced by the generation of a proton, in proximity of an electrode [9, 10]. The electron is affixed to the DNA molecule and does not move. However, the proton diffuses away, causing a change in the polarization of the electrode, resulting in a transient current that may be detected by an integrating amplifier.

For the detection method discussed in this paper, the probe and target oligonucleotide must not be the same length because we detect the incorporation of nucleotides into the double-stranded sequence during polymerization. This is not problematic because target sequences are generally longer than their corresponding probes. As an example in Figure 1, the next base to be incorporated is an "A" as indicated by the dotted lines. When the polymerase enzyme incorporates the "A" into the DNA backbone, we measure a transient current on the electrode. Although detection of oligonucleotides in a biological sample is one obvious application of this technique, it may also be used to sequence a short segment of DNA by introducing nucleotides sequentially with intermediate wash steps.

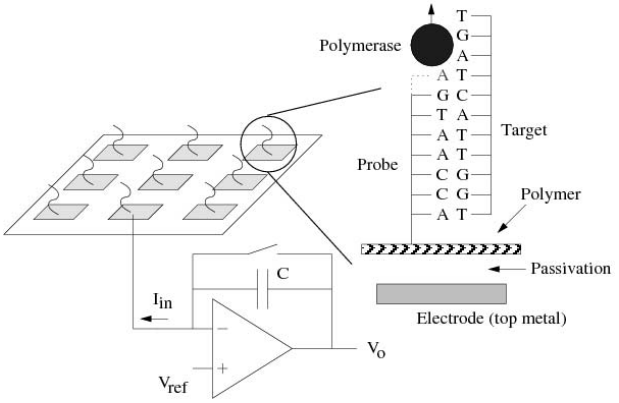

Fig. 1. Detection principle and schematic of system. As the polymerase enzyme incorporates a nucleotide (an "A") into the DNA to form a double helix, an unbound proton diffuses away, leaving an electron affixed to the DNA backbone. A compensating charge is thus induced on the sensing electrode, which accumulates on an integration capacitor.

III. INDUCED CHARGE

The DNA polymerization sensing technique discussed in this paper is based on a charge measurement, arising from the diffusion of many protons away from an electrode. We are interested in determining the total induced charge arising from this diffusion process. Let us first consider compute the amount of charge induced on an electrode of dimensions w by w square-units by a single point charge of charge q located above the electrode surface as shown in the inset to Figure 2. Let the coordinate z-axis pass through the center of the electrode, and let the single-point charge be located at (x, y, z). From Maxwell's equations, a single point charge induces a surface charge density of

$$\rho_s = \frac{-qz}{2\pi \left(x^2 + y^2 + z^2\right)^{\frac{3}{2}}} \tag{1}$$

on an infinite, planar electrode surface [11]. We approximate the charge induced on a finite electrode by using the induced charge density for an infinite, planar electrode. The total charge induced, Q_{ind}, on a planar electrode from a single point charge at (x, y, z) may therefore be approximated as

$$Q_{ind}\left(x, y, z\right) = \int_{-\frac{w}{2}-y}^{\frac{w}{2}-y} \int_{-\frac{w}{2}-x}^{\frac{w}{2}-x} \rho_s\left(x', y'\right) dx' dy'. \tag{2}$$

Integrating for the total induced charge yields the solution

$$\begin{aligned} Q_{ind}\left(x, y, z\right) = -\frac{q}{2\pi} \Big[& \Lambda\left(\frac{w}{2} - x, \frac{w}{2} - y\right) + \\ & \Lambda\left(\frac{w}{2} - x, \frac{w}{2} + y\right) + \Lambda\left(\frac{w}{2} + x, \frac{w}{2} - y\right) \\ & + \Lambda\left(\frac{w}{2} + x, \frac{w}{2} + y\right)\Big] \end{aligned} \tag{3}$$

$$\Lambda\left(x, y\right) = \arctan \frac{xy}{z\sqrt{x^2 + y^2 + z^2}}$$

Figure 2 shows the induced charge versus charge position coordinates normalized by the electrode width, i.e. $\left(\frac{x}{w}, \frac{y}{w}, \frac{z}{w}\right)$. Note that the electrode ranges from $-\frac{1}{2} \leq x, y \leq \frac{1}{2}$. As a charge moves in a plane which is 1% of the electrode width above the electrode, nearly all of the charge is induced on the electrode; in this case for electrons directly above the electrode, the electrode is essentially an infinite plane.

As hydrogen ions diffuse away from the electrode where they are generated, a transient current is generated at the electrode. This transient current flows through an integrating capacitor which compensates for the induced electrode charge as shown in Figure 2. Our DNA molecules will be tethered close to the electrode in order to maximize the induced charge.

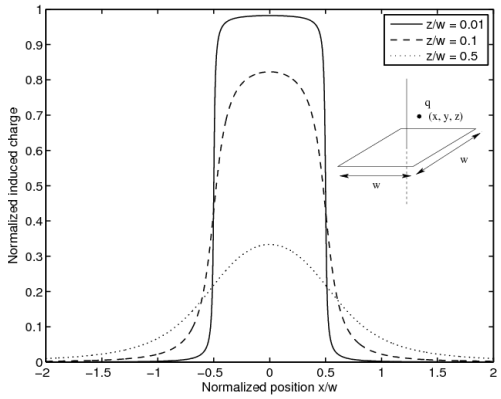

Fig. 2. Induced charge versus $\frac{x}{w}$ along $y = 0$ for several fixed values of $\frac{z}{w}$.

IV. ARCHITECTURE

We designed an integrated circuit containing an array of electrodes, integrating amplifiers (directly under each electrode), and reset circuitry. The operational transconductance amplifier (OTA) in our sensor uses a folded cascode topology with gain-boosting in a $0.18\ \mu$m standard CMOS process. Gain boosting amplifiers are used to increase the gain of the cascode transistors [12]. The gain boosting amplifiers are also implemented with a folded cascode architecture, and the total simulated OTA gain is 110 dB. Figures 3 and 4 show the architecture of the main, gain-boosting, and common mode feedback OTAs.

Because DNA polymerization is detected simultaneously for all pixels, there is a single reset clock for all integration capacitors. The reset clock is provided off-chip in order to coordinate introduction of nucleotides with signal measurement.

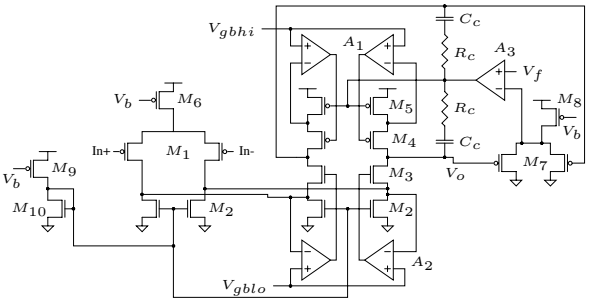

Fig. 3. A transistor level schematic of the main OTA used in each pixel.

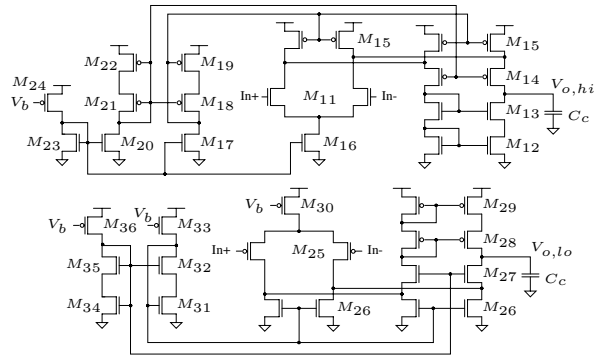

Fig. 4. Transistor level schematics of the gain boosting and common-mode feedback OTAs, which are used to increase the overall gain of the main OTA. The top OTA corresponds to A_1 in the main OTA circuit while the bottom OTA corresponds to A_2 and A_3.

Power dissipation needs to be somewhat limited in order to prevent the surface temperature of the die from rising significantly and affecting enzyme activity. The total power consumption was 44 mW with all 25 pixels active, and we measured a 0.5 °C rise in surface temperature above ambient for our chip.

The sensing electrodes are fabricated in the top metal of a 0.18 μm standard CMOS process; they are 300 μm square on a 500 μm pitch. Although the active sensor array occupies an area of 5.3 mm^2, the actual chip area is significantly larger because it must be manually surrounded by epoxy to isolate the bondwires. The OTA and 30 pF integration capacitor are placed below the electrode in each pixel. In order to mitigate problems caused by antenna effects during fabrication, the amplifier uses double gate oxide devices which operate from a 3.3 V supply. The passivation layer used to encapsulate the die covers the electrodes (only removed from the bondpads). Unlike previous work [2–4], our sensors do not require additional post-processing to obtain gold electrodes or GMR structures

Technology	0.18 μm CMOS
Active Sensor Area per Pixel	0.09 mm^2
Surface Temperature Rise‡	0.5 °C above ambient
Nominal Gain†	110 dB
Gain($V_o = +1$ V)†	63 dB
Gain($V_o = -1$ V)†	82 dB
Unity Gain Frequency†	250 kHz
Phase Margin†	75°
CMRR†	110 dB
Power per Pixel‡	1.8 mW
Input-referred OTA voltage noise†	22 nV/$\sqrt{\text{Hz}}$
K_f ($\frac{1}{f}$-noise constant)‡	1.2×10^{-10} V^2

TABLE I. OTA Specifications. † indicates simulated for the typical process corner. ‡ indicates measured.

on the surface of our die. To attach DNA probes, a thin polymer layer is applied on top of the die passivation and single-stranded DNA probes are placed above each electrode by spotting. Figure 5 shows a picture of the die with a 5x5 array of electrode/amplifier pixels.

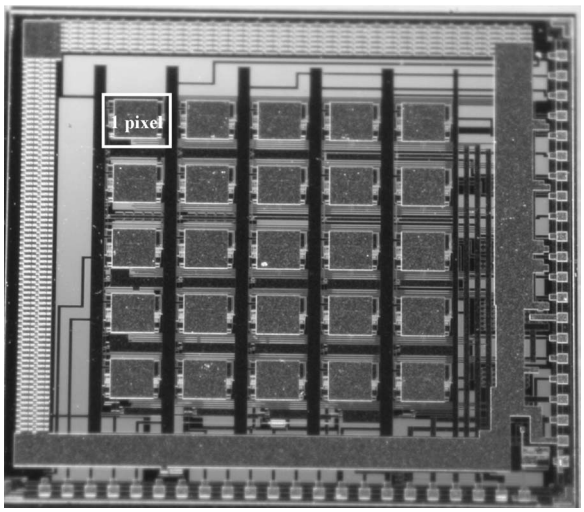

Fig. 5. Die photograph.

V. NOISE

Because noise ultimately determines the smallest detectable signal, in this section, we calculate the various electronic noise contributions from the OTA which appear at the sensor output. Because we are sensing a transient phenomena, we perform a noise analysis in the time domain. At the output of the OTA, there will be contributions from the input-referred thermal OTA current and voltage noise, $\frac{1}{f}$-noise, shot noise, and reset noise of the integration capacitor.

A. Thermal voltage noise

Here we calculate the temporal output noise contribution, $E\left[V_{oV}\left(t_{int}\right)\right]^2$, arising from the input-referred voltage noise at the end of the integration period. Let $\overline{V_n^2}$ denote the input-referred thermal voltage noise of the OTA in units of $\mathrm{V}^2/\ \mathrm{Hz}$. The voltage-noise versus frequency at the sensor output is

$$V_{oV} = \frac{A_o\sqrt{\overline{V_n^2}}}{A_o + 1 + j\frac{\omega_o}{\omega}} \tag{4}$$

where the OTA has a single-pole behavior with a DC gain of A_o and a pole frequency of ω_o. The temporal contribution of the thermal output voltage noise $E\left[V_{oV}\left(t_{int}\right)\right]^2$ is equal to the autocorrelation of the output thermal voltage noise, R_{V_o}, evaluated at time $\tau = 0$

$$\begin{aligned} E\left[V_{oV}\left(t_{int}\right)\right]^2 &= R_{V_{oV}}\left(0\right) = \\ &= \frac{1}{2\pi}\int_{-\infty}^{\infty}\frac{A_o^2\omega_o^2\overline{V_n^2}}{\left(A_o+1\right)^2\omega_o^2+\omega^2}\,d\omega \\ &= \frac{A_o^2\omega_o\overline{V_n^2}}{2\left(A_o+1\right)} \approx \frac{A_o\omega_o\overline{V_n^2}}{2}. \end{aligned} \tag{5}$$

Note that the temporal output-referred voltage noise is proportional to the gain-bandwidth product of the OTA. Using the simulated numbers from the typical process corner, with an OTA input-referred voltage noise of 22 $\mathrm{nV}/\sqrt{\mathrm{Hz}}$ and a gain-bandwidth product of 250 kHz, the noise contribution at the OTA output is 7.8 μV.

B. $\frac{1}{f}$-noise

An analysis similar to the thermal noise case may be performed to obtain the sensor output noise contribution for $\frac{1}{f}$- or flicker noise

$$E\left[V_{o\frac{1}{f}}\left(t_{int}\right)\right]^2 \approx 2K_f\ln\left[\frac{\omega_{max}}{\omega_{min}}\right] \tag{6}$$

given a band-limited noise contribution of

$$S_{\frac{1}{f}} = \begin{cases} \frac{K_\omega}{\omega} & \omega_{min} < |\omega| < \omega_{max} \\ 0 & \text{otherwise} \end{cases}. \tag{7}$$

Note that we use $K_\omega = 2\pi K_f$. Given a measured $K_f = 1.2\times 10^{-10}\ \mathrm{V}^2$, $f_{max}/f_{min} = 2.5\times 10^5$, the output flicker noise contribution is 55 μV.

C. Thermal current and Shot Noise

Here we calculate the temporal output noise, $E\left[V_{oI}\left(t_{int}\right)\right]^2$, at the output after an integration of t_{int} seconds. Let $\overline{I_n^2}$ denote the input-referred current noise in units of $\mathrm{A}^2/\ \mathrm{Hz}$. The current noise contribution at the output is given by

$$\begin{aligned} E\left[V_{oI}\left(t_{int}\right)\right]^2 &= E\int_0^{t_{int}}\int_0^{t_{int}}\frac{I_n\left(t\right)I_n\left(s\right)}{C^2}\,dt\,ds \\ &= \int_0^{t_{int}}\int_0^{t_{int}}\frac{\overline{I_n^2}\delta\left(t-s\right)}{C^2}\,dt\,ds \\ &= \frac{\overline{I_n^2}t_{int}}{C^2}. \end{aligned} \tag{8}$$

Equation 8 gives an expression for how much shot noise appears at the output if $\overline{I_n^2}$ is replace by $2qI_{avg}$ where I_{avg} is the average current flowing through the integration capacitor. For an OTA input-referred current noise of 1 $\mathrm{fA}/\sqrt{\mathrm{Hz}}$, an integration time of 100 ms, an average input current of 1 pA, and an integration capacitance of 30 pF, the output noise contribution is 10.5 μV from the thermal current noise and 6.0 μV from the shot noise.

D. Total Noise

Combining the noise contributions calculated above, we obtain the total output noise

$$\begin{aligned} \overline{V_o^2} = &\frac{A_o\omega_o\overline{V_n^2}}{2} + 2K_f\ln\left(\frac{\omega_{max}}{\omega_{min}}\right) + \\ &+ \frac{\left(\overline{I_n^2}+2qI_{avg}\right)t_{int}}{C^2} + \frac{kT}{C} + \overline{V_{buf}^2} \end{aligned} \tag{9}$$

where k is Boltzmann's constant, T is the temperature in Kelvin, t_{int} is the signal integration time, A_o is the DC gain of a single pole OTA with pole frequency ω_o, and $\overline{I_n^2}$ and $\overline{V_n^2}$ are respectively the input-referred thermal current and voltage noise of the OTA in units of $\mathrm{A}^2/\ \mathrm{Hz}$ and $\mathrm{V}^2/\ \mathrm{Hz}$. Note that we have also included noise from resetting of the integration capacitor, which at 300 K contributes 12 μV of noise. Furthermore, we have included a noise contribution from the enzymatic buffer, $\overline{V_{buf}^2}$. This model predicts the measured sensor noise very accurately from the electronics (without the enzymatic buffer). We will see later in Sections VI and VII that the enzymatic buffer noise contribution dominates that from the sensing electronics by roughly a factor of four.

VI. THE AMPLIFIER AS A CHARGE SENSOR

Above, we described the CMOS circuit as an integrator. The circuit may also be understood as a charge sensor, and we discuss this interpretation in this section. Let Q denote the charge on the electrode connected to the input of the OTA. Assume that at time 0^-, the capacitor C has been reset so that the voltage across the capacitor is zero. One question is: how small of

a change in charge can the sensor detect? If we define the minimum detectable charge differential as the amount of charge required to cause the output voltage to be equal to one standard deviation of the noise voltage, we obtain using Equation 9,

$$\Delta Q = \sqrt{C^2\overline{V_{buf}^2} + \frac{A_o\omega_o\overline{V_n^2}C^2}{2} + 2K_fC^2\ln\left(\frac{\omega_{max}}{\omega_{min}}\right) + \\ + kTC + \left(\overline{I_n^2} + 2qI_{avg}\right)t_{int}}\,. \quad (10)$$

Note that minimizing the integrating capacitor minimizes the detectable charge differential. However, decreasing the integration capacitance causes the output voltage to saturate faster for a fixed input current. In order to acquire an adequate quantity of samples to display the transient nature of the pulse, we choose not to minimize the capacitance (acceptable because the enzymatic buffer noise dominates that from the electronics). We measured the minimum detectable charge differential from the electronics alone (ignoring the enzymatic buffer) to be 7 fC at 300 K. Note that this input charge noise can be reduced by decreasing the integration capacitance; a 300 fF integration capacitance results in a reduction in the noise by 100x, but would also saturate 100x faster. In practice, the minimum detectable charge differential is larger because the noise from the enzymatic buffer dominates the contributions from the amplifier.

VII. THE AMPLIFIER AS A CURRENT SENSOR

As mentioned above, the sensor may be thought of as detecting a transient current. In this section, we explore the total noise as if it originated solely from a current source at the amplifier input.

Defining the minimum detectable input current as the input current level which results in SNR $= 1$, we have

$$I_{min} = \frac{C}{t_{int}}\sqrt{\overline{V_o^2}} \\ = \left[\frac{C^2\overline{V_{buf}^2}}{t_{int}^2} + \frac{A_o\omega_o\overline{V_n^2}C^2}{2t_{int}^2} + \frac{2K_fC^2}{t_{int}^2}\ln\left(\frac{\omega_{max}}{\omega_{min}}\right) + \right. \\ \left. + \frac{kTC}{t_{int}^2} + \frac{\overline{I_n^2} + 2qI_{avg}}{t_{int}}\right]^{\frac{1}{2}}. \quad (11)$$

Because input current limits are transient and have a finite width in time, say t_{int}, Equation 11 gives a limit on the smallest current that may be detected by the amplifier. The faster the transient current, the higher the minimum detectable current. One trend that we note is that the minimum detectable current increases with the integration capacitance.

Figure 6 shows the experimental minimum detectable current versus integration time with and without the enzymatic buffer. A grounded Ag/Cl electrode was placed in the enzymatic buffer during noise measurements. The lower curve is the measured minimum detectable current without an enzymatic buffer, which precisely agrees with the predicted value using Equation 11 and Table I. We may observe that the minimum detectable current with a buffer solution on the integrated circuit is roughly a factor of 4 times higher than without the buffer. Thus, the dominant noise source in the system comes from the enzymatic buffer, not the measurement circuit. For an integration time of 1 second, the minimum detectable current is 7 fA without the buffer and 25 fA with it. Because the noise due to the electronics alone is not the dominant noise contribution, techniques such as correlated double sampling would not be an effective noise reduction technique for our application.

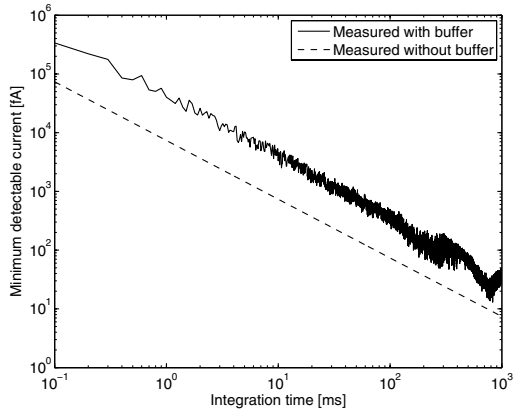

Fig. 6. The measured minimum detectable current versus integration time. The lower line represents the detection floor set by the noise of the electronics.

VIII. SURFACE MODIFICATION OF CMOS CHIPS

The integrated circuits were glued in a leadless chip carrier socket, and bondwires were used to connect the integrated circuit to the socket. Epoxy encapsulated the bondwires and also formed a well on top of the integrated circuit (to contain the enzymatic buffer solution). Then they were cleaned by washing with acetone and iso-propanol for 1 minute each followed by a 3 minute exposure to UV-ozone using a UVO cleaner. The sensor chips were then immersed in a 5% (w/w) (chloromethyl)phenylethyltrimethoxysilane in ethanol solution with gentle shaking for 12 hours. The chips were then rinsed with ethanol three times and dried in air. A 100 μM solution of probe oligonucleotides in phosphate buffer saline at pH 7.4 (0.01 M sodium phosphate, 1.0 M NaCl) was manually spotted onto the microchips and kept in a humid chamber overnight, immobilizing the probes above the electrodes. The probe oligonucleotides used in this study have the sequence: 5'–NH_2–C_{12}–TTT TTT TTT TTG TGC CAA GTA CAT ATG ACC CTA CT–3'. After washing away unattached probes in DI water, the chips were blocked with 50 mM ethanolamine solution for 2 hours at room temperature.

Target oligonucleotides at a concentration of 500 nM in a PBS buffer at pH 7.4 (sodium phosphate 0.01 M, NaCl 0.3 M) were hybridized onto the sensor chips overnight, rinsed with PBS buffer, and dried before measurements. The target oligonucleotides had the sequence: 5'–ATG CGG CAG AGC AGT GAG CTC AGC ATG TCC ATA CCA GTA GGG TCA TAT GTA CTT GGC AC–3'.

IX. MEASURED DNA POLYMERIZATION SIGNAL

After surface preparation, we measured the DNA polymerization signal from our CMOS chip. Twenty μL of a polymerization buffer containing 1.25 mM $MgCl_2$, 20 mM KCl, 5 mM Tris-HCl (pH 8.5) and 5 U Klenow exo- (Fermentas) were dispensed onto the electrodes of the CMOS chip. The buffer was allowed to equilibrate for 5 minutes, and then 2 μL dNTP solution (dATP, dTTP, dCTP, and dGTP so that multiple nucleotides are incorporated) was introduced onto the surface of the chip while the output voltage was recorded. A LabView program coordinated the release of the dNTPs with data acquisition. Figure 7 shows the resulting signal for electrodes with and without immobilized DNA. The initial voltage spikes on both channels result from the introduction of dNTPs into the solution above the electrodes. The output voltage from the electrode with immobilized DNA rises to 150 mV whereas the output voltage from the electrode without immobilized DNA settles back to a value slightly above the initial baseline, confirming that polymerization of a complementary target occurred at the electrode with immobilized DNA.

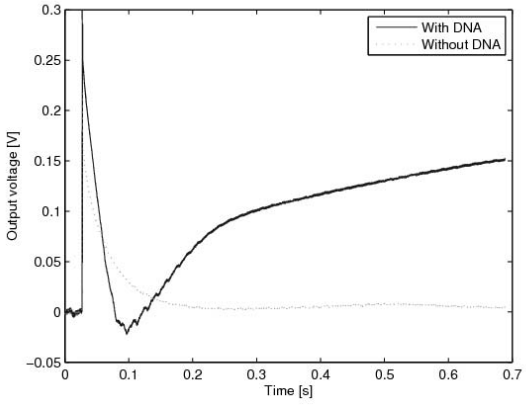

Fig. 7. Measured signal from electrodes with and without immobilized DNA probes (same chip). The voltage at the electrode with immobilized DNA results from a charge induced on the sensing electrodes. The initial voltage spikes for electrodes with and without immobilized DNA result from introduction of nucleotides into the solution above the electrodes.

X. CONCLUSIONS

We described the first CMOS DNA polymerization sensor. The sensor could be used to sequence short DNA segments in addition to detecting DNA hybridization in microarrays. The measured limit of detection (with enzymatic buffer) is 25 fA for a one second integration time, or equivalently 25 fC of charge. By comparison, the electronic-noise limit of detection is 7 fA for a one second integration time, or equivalently 7 fC of charge, rendering further reduction in electronic noise unnecessary. Using our chip, we demonstrate the detection of DNA polymerization.

ACKNOWLEDGEMENT

The authors would like to thank Miloslav Karhanek for his valuable feedback.

REFERENCES

[1] M. Barbaro, A. Bonfiglio, L. Raffo, A. Alessandrini, P. Facci, and I. Barak. A CMOS, fully integrated sensor for electronic detection of DNA hybridization. *IEEE Electron Device Letters*, 27(7):595 – 597, July 2006.

[2] C. Stagni, C. Guiducci, L. Benini, B. Ricco, S. Carrara, C. Paulus, M. Schienle, and R. Thewes. A fully electronic label-free DNA sensor chip. *IEEE Sensors Journal*, 7(4):577 – 585, 2007.

[3] M. Schienle, C. Paulus, A. Frey, F. Hofmann, B. Holzapfl, P. Schindler-Bauer, and R. Thewes. A fully electronic DNA sensor with 128 positions and in-pixel A/D conversion. *IEEE Journal of Solid-State Circuits*, 39(12):2438 – 2445, December 2004.

[4] Y. T. Cheng, C. Y. Tsai, and P. H. Chen. Development of an integrated CMOS DNA detection biochip. *Sensors and Actuators, B: Chemical*, 120(2):758 – 765, Jan 2007.

[5] S. Han, H. Yu, B. Murmann, and S. Wang. A high-density magnetoresistive biosensor array with drift-compensation mechanism. In *IEEE International Solid-State Circuits Conference; Feb 11-15 2007; San Francisco, CA, United States*, pages 168 – 169.

[6] J. Li, M. Xue, Z. H. Lu, Z. K. Zhang, C. Feng, and M. Chan. A high-density conduction-based micro-DNA identification array fabricated with a CMOS compatible process. *IEEE Transactions on Electron Devices*, 50(10):2165 – 2170, October 2003.

[7] A. Poghossian, A. Cherstvy, S. Ingebrandt, A. Offenhausser, and M. J. Schoning. Possibilities and limitations of label-free detection of DNA hybridization with field-effect-based devices. *Sensors and Actuators B*, 111 – 112(SUPPL.):470 – 480, Nov 2005.

[8] J. S. Daniels and N. Pourmand. Label-free impedance biosensors: Opportunities and challenges. *Electroanalysis*, 19(12):1239 – 1257, May 2007.

[9] N. Pourmand, M. Karhanek, H. H. J. Persson, C. D. Webb, T. H. Lee, A. Zahradnikova, and R. W. Davis. Direct electrical detecion of DNA synthesis. *Proceedings of the National Academy of Science*, 103(17):6466 – 6470, Apr 25, 2006.

[10] E. P. Anderson, J. S. Daniels, H. Yu, M. Karhanek, T. H. Lee, R. Davis, and N. Pourmand. A system for multiplexed direct electrical detection of DNA synthesis. *Sensors and Actuators B*, 129(1):79 – 86, Jan 2008.

[11] Matthew N. O. Sadiku. *Elements of Electromagnetics*. Oxford Univ Press, Oxford, UK, third edition, 2000.

[12] K. Bult and G. J. Geelen. A fast-settling CMOS op amp for SC circuits with 90-dB DC gain. *IEEE Journal of Solid-State Circuits*, 25(6):1379 – 1384, Dec 1990.

[13] A. Hassibi and T. H. Lee. A programmable 0.18-μm CMOS electrochemical sensor microarray for biomolecular detection. *IEEE Sensors Journal*, 6(6):1380 – 1388, December 2006.